

Evolutionary Pareto Set Learning with Structure Constraints

Xi Lin, Xiaoyuan Zhang, Zhiyuan Yang, Qingfu Zhang, *Fellow, IEEE*

Abstract—The multiobjective evolutionary optimization algorithm (MOEA) is a powerful approach for tackling multiobjective optimization problems (MOPs), which can find a finite set of approximate Pareto solutions in a single run. However, under mild regularity conditions, the Pareto optimal set of a continuous MOP could be a low dimensional continuous manifold that contains infinite solutions. In addition, structure constraints on the whole optimal solution set, which characterize the patterns shared among all solutions, could be required in many real-life applications. It is very challenging for existing finite population based MOEAs to handle these structure constraints properly. In this work, we propose the first model-based algorithmic framework to learn the whole solution set with structure constraints for multiobjective optimization. In our approach, the Pareto optimality can be traded off with a preferred structure among the whole solution set, which could be crucial for many real-world problems. We also develop an efficient evolutionary learning method to train the set model with structure constraints. Experimental studies on benchmark test suites and real-world application problems demonstrate the promising performance of our proposed framework.

Index Terms—Multiobjective Optimization, Evolutionary Algorithm, Pareto Set Learning, Structure Constraint.

I. INTRODUCTION

MULTIOBJECTIVE optimization problems (MOPs) naturally arise in many real-world applications, from engineering design [1] to machine learning [2], [3]. In this paper, we consider the following continuous multiobjective optimization problem:

$$\min_{\boldsymbol{x} \in \mathcal{X}} \boldsymbol{F}(\boldsymbol{x}) = (f_1(\boldsymbol{x}), f_2(\boldsymbol{x}), \dots, f_m(\boldsymbol{x})), \quad (1)$$

where \boldsymbol{x} is the decision variable in the decision space $\mathcal{X} \subset \mathbb{R}^n$ and $\boldsymbol{f} : \mathbb{R}^n \rightarrow \mathbb{R}^m$ consists of m objective functions. Very often, these objective functions conflict one another, and no single solution \boldsymbol{x} can optimize all the objectives at the same time. Instead, there is a set of Pareto optimal solutions with different optimal trade-offs among objectives. Under mild conditions, the set of all Pareto optimal solutions (called the Pareto set) and its image in the objective space (called the Pareto front) are both $(m - 1)$ -dimensional piecewise continuous manifolds in the decision space and objective space, respectively [4], [5].

Over the past three decades, many multiobjective optimization algorithms have been proposed to find a single or a finite set of Pareto optimal solutions with different trade-offs among all objectives [6], [7]. Among them, the multiobjective

evolutionary algorithms (MOEA) [8], [9], [10] is a widely-used methodology to produce a finite set of approximate Pareto optimal solutions in a single run. However, a finite set of solutions cannot always approximate the whole Pareto set very well. In many real-world applications, it could be very difficult for decision-makers to extract their desired information from a finite set of approximate Pareto solutions to make final decisions. Many model-based methods have been proposed to assist or improve traditional MOEAs, such as surrogate-assisted optimization [11], [12], [13], model-based preference assignment [14], [15], [16], hypervolume approximation [17], [18] and Pareto set/front approximation from a finite set of solutions [19], [4], [5], [20], [21], [22].

Recently, we have developed a one-stage Pareto set learning (PSL) framework [23], [24], [25], [26] to approximate the whole Pareto set simultaneously, which does not require approximate Pareto optimal solutions in advance. With gradient-based training method, it can learn the Pareto optimal set for deep multi-task learning [27], [28], [29], neural multiobjective combinatorial optimization [23], expensive multiobjective optimization [24], and multiobjective diverse graph generation [30]. In this paper, we extend the PSL framework to solve black-box MOPs with an efficient evolutionary stochastic optimization method, which is called evolutionary Pareto set learning (EPSL). EPSL naturally generalizes the decomposition-based MOEA (MOEA/D) [31] from a finite population to a parameterized math model. With the learned model, decision-makers can readily obtain approximate Pareto optimal solutions for any preferences.

In many real-world applications, it could be desirable to add some structure constraints on the optimal solution set. For example, in multiobjective modular design [32], [33], the production cost can be significantly reduced if the solutions (i.e., design schemes) for different scenarios share some common components. Innovation proposed and advocated by Deb et al.[34], [35], [36], [37], [38] aims at mining useful patterns among different Pareto optimal solutions for decision making, which is conducted as post-optimization analysis. In this paper, we propose a different method to actively incorporate decision-maker-preferred structure patterns into the whole solution set. In a sense, our method can be regarded as a model-based approach for innovation that actively incorporates predefined structure patterns as prior. Using our proposed method, the Pareto optimality of the solution set can now be traded off with the desirable structure constraint. We believe it is necessary to go beyond Pareto optimality in multiobjective optimization and consider other user requirements on common solution patterns in the optimization process.

Xi Lin, Xiaoyuan Zhang, Zhiyuan Yang, and Qingfu Zhang are with the Department of Computer Science, City University of Hong Kong, Hong Kong SAR, China (email: xi.lin@my.cityu.edu.hk, qingfu.zhang@cityu.edu.hk).

Our main contributions can be summarized as follows:

- We propose a novel evolutionary learning method to learn the whole solution set for black-box MOPs, which uses the same information and evaluation budget for a typical MOEA.
- We make a first attempt to add different decision-maker-defined structure constraints on the whole solution set for multiobjective optimization.
- We experimentally compare EPSL with other representative MOEAs on different multiobjective engineering optimization problems, and also validate its ability to deal with structure constraints. The results confirm the effectiveness and usefulness of EPSL for solving MOPs.

II. EVOLUTIONARY PARETO SET LEARNING

In this section, we first introduce some basic concepts and the Pareto set learning model recently proposed by us [23], [24], and then propose a lightweight evolutionary stochastic optimization algorithm for efficient model training.

A. Basic Definitions

For a multiobjective optimization problem (1), we have the following definitions:

Definition 1 (Pareto Dominance). *Let $\mathbf{x}^a, \mathbf{x}^b \in \mathcal{X}$ be two candidate solutions for the multiobjective optimization problem (1), \mathbf{x}^a is said to dominate \mathbf{x}^b , denoted by $\mathbf{x}^a \prec \mathbf{x}^b$ if and only if $f_i(\mathbf{x}^a) \leq f_i(\mathbf{x}^b), \forall i \in \{1, \dots, m\}$ and $f_j(\mathbf{x}^a) < f_j(\mathbf{x}^b), \exists j \in \{1, \dots, m\}$.*

Definition 2 (Strict Dominance). *Let $\mathbf{x}^a, \mathbf{x}^b \in \mathcal{X}$, \mathbf{x}^a is said to strictly dominate \mathbf{x}^b , denoted by $\mathbf{x}^a \prec_{strict} \mathbf{x}^b$, if and only if $f_i(\mathbf{x}^a) < f_i(\mathbf{x}^b), \forall i \in \{1, \dots, m\}$.*

Definition 3 (Pareto Optimality). *A solution $\mathbf{x}^* \in \mathcal{X}$ is Pareto optimal if there does not exist $\mathbf{x} \in \mathcal{X}$ such that $\mathbf{x} \prec \mathbf{x}^*$. The set of all the Pareto optimal solutions is called the Pareto set, denoted by PS, and its image $\mathbf{f}(PS)$ in the objective space is called the Pareto front (PF).*

Definition 4 (Weakly Pareto Optimality). *A solution $\mathbf{x}' \in \mathcal{X}$ is weakly Pareto optimal if there does not exist $\hat{\mathbf{x}} \in \mathcal{X}$ such that $\hat{\mathbf{x}} \prec_{strict} \mathbf{x}'$. The weakly Pareto set/front can be defined accordingly.*

For a continuous MOP (1), under mild conditions, the Pareto set is an $(m - 1)$ -dimensional manifold which consists of an infinite number of solutions [4], [5], [7]. In other words, it is natural and feasible to use a math model to represent the PS.

B. Aggregation Methods

Let $\boldsymbol{\lambda} \in \Delta$ be a weight vector on the simplex $\Delta = \{\boldsymbol{\lambda} = (\lambda_1, \dots, \lambda_m)^T \in \mathbb{R}_+^m | \sum_{i=1}^m \lambda_i = 1\}$, aggregation methods [7] combine all the individual objectives into one single objective function and optimize it to obtain one single Pareto optimal solutions. The most widely-used weighted-sum aggregation works as follows:

$$g_{ws}(\mathbf{x}|\boldsymbol{\lambda}) = \sum_{i=1}^m \lambda_i f_i(\mathbf{x}). \quad (2)$$

It is well-known that the weighted-sum aggregation method is not able to find some Pareto optimal solutions when the PF is not convex. Many other aggregation methods have been developed to overcome this shortcoming over the past several decades [39], [31], [40], [41], [42]. In this paper, we adopt the weighted Tchebycheff aggregation approach [43], and our work can be readily generalized to other aggregation methods. The Tchebycheff-aggregated single objective function is defined as:

$$g_{tch}(\mathbf{x}|\boldsymbol{\lambda}) = \max_{1 \leq j \leq m} \{\lambda_j (f_j(\mathbf{x}) - (z_j^* - \varepsilon))\}, \quad (3)$$

where $z_j^* = \min_{\mathbf{x} \in \mathcal{X}} f_j(\mathbf{x})$ is an ideal value for the i -th objective, $\varepsilon > 0$ is a small positive component, and $(z_j^* - \varepsilon)$ is also called an (unattainable) utopia value for the i -th objective. The necessary and sufficient condition for Tchebycheff aggregation to obtain the whole Pareto set is

Theorem 1 (Theorem 4.24 in [6] which is a modified version from [44]). *A feasible solution $\mathbf{x} \in \mathcal{X}$ is weakly Pareto optimal for the multiobjective optimization problem if and only if there is a weight vector $\boldsymbol{\lambda} > 0$ such that \mathbf{x} is an optimal solution of the Tchebycheff aggregation subproblem (3).*

In other words, all weakly Pareto solutions \mathbf{x}^* can be found by solving the Tchebycheff scalarized subproblem with a specific weight vector $\boldsymbol{\lambda}$. This result suggests that we can use the weight vector $\boldsymbol{\lambda} \in \Delta$ to parameterize the PS.

Many classic optimization methods have been proposed to find a single Pareto optimal solution by optimizing a single-objective aggregation function [6], [7], while multiobjective evolutionary algorithms (MOEAs) [8], [9], [10] can find a number of different Pareto optimal solutions in a single run. Among them, the decomposition-based MOEAs (MOEA/D) [31], [45] use an aggregation method to decompose a MOP into a finite number of single objective subproblems with different weight vectors and solve them in a collaborative manner. This paper generalizes MOEA/D to produce optimal solutions for all the weight vectors via a single model.

C. Pareto Set Model

We propose to model the whole Pareto set as:

$$\mathbf{x} = h_{\theta}(\boldsymbol{\lambda}), \quad (4)$$

where $\boldsymbol{\lambda} \in \Delta$, and $h_{\theta} : \Delta \rightarrow \mathcal{X}$ is a model with learnable parameter $\theta \in \Theta$. Our task is to learn an optimal θ^* such that $\mathbf{x}^* = h_{\theta^*}(\boldsymbol{\lambda})$ is the optimal solution to

$$\min_{\mathbf{x} \in \mathcal{X}} g_{tch}(\mathbf{x}|\boldsymbol{\lambda}), \quad \forall \boldsymbol{\lambda} \in \Delta. \quad (5)$$

Let $P(\boldsymbol{\lambda})$ be a user-specific probability distribution for $\boldsymbol{\lambda}$, then our task can be defined as:

$$\min_{\theta \in \Theta} L(\theta) = E_{\boldsymbol{\lambda} \sim P(\cdot)} g_{tch}(h_{\theta}(\boldsymbol{\lambda})|\boldsymbol{\lambda}). \quad (6)$$

In this paper, h_{θ} is set to be a two-layer fully-connected neural network where θ is its model parameters, and well-developed neural network training algorithms can be naturally used for learning the Pareto set model.

We would like to make the following remarks on the Pareto set learning problem (6):

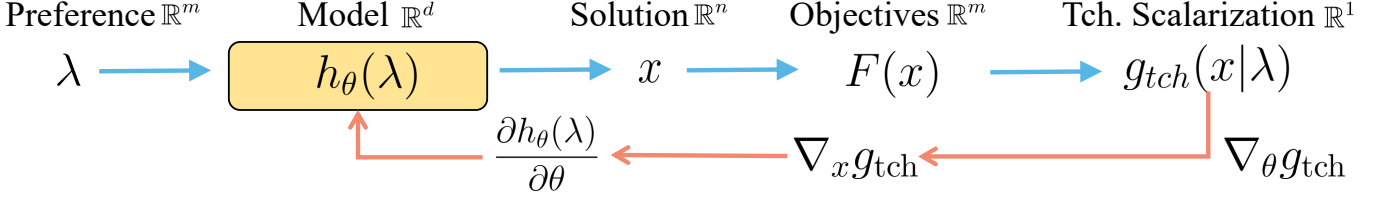


Fig. 1. **Evolutionary Pareto Set Learning (EPSL): (a) The forward pass** (\rightarrow) starts from the preference $\lambda \in \mathbb{R}^m$ to the model $h_\theta(\lambda)$ with parameter $\theta \in \mathbb{R}^d$ to the solution $x \in \mathbb{R}^n$ to the objectives $F(x) \in \mathbb{R}^m$ and finally to the preference-conditioned subproblem scalar $g_{\text{tch}}(x|\lambda) \in \mathbb{R}^1$. The learnable **model parameter** θ is the only variable to optimize in this model. **(b) The backward gradient** $\nabla_\theta g_{\text{tch}}$ (\leftarrow) from the subproblem scalar $g_{\text{tch}}(x|\lambda) \in \mathbb{R}^1$ with respect to the learnable model parameter $\theta \in \mathbb{R}^d$ can be decomposed into a low-dimensional gradient $\nabla_x g_{\text{tch}}$ and a high-dimensional Jacobian matrix $\frac{\partial h_\theta(\lambda)}{\partial \theta}$, where the first term can be efficiently estimated by evolution strategies and the second term can be directly calculated by backpropagation.

- If $P(\lambda)$ is a uniform distribution on a finite number of weight vectors, problem (6) is equivalent to the task of MOEA/D, that is, to optimize a finite number of aggregated functions at the same time.
- Problem (6) is for optimizing model parameter θ instead of decision variable x . Even when objectives f_i are not differentiable or their gradients are not available, it is still possible to compute or estimate the gradient of $L(\theta)$. Therefore, efficient gradient search methods can be used for optimizing problem (6).
- $P(\lambda)$ can be set to suit the decision-maker's preferences. For example, if the decision-maker is interested in only a preference subset, $P(\lambda)$ can be set in such a way that its supporting set is this preference subset in problem (6).
- Although this work focuses on continuous MOPs, our modeling approach can also tackle combinatorial problems by reformulating them into single-objective continuous model learning [23].

D. Evolutionary Stochastic Optimization

It is very difficult to directly solve the optimization problem (6) since the expected term in $L(\theta)$ cannot be exactly computed in most cases. Treating it as a stochastic optimization problem [46], [47], [48], we propose to use stochastic gradient descent methods for learning the Pareto set model. At each iteration, $L(\theta)$ is approximated via Monte Carlo sampling:

$$\tilde{L}(\theta) = \frac{1}{N} \sum_{i=1}^N g_{\text{tch}}(h_\theta(\lambda^i)|\lambda^i), \quad (7)$$

where $\{\lambda^1, \lambda^2, \dots, \lambda^N\}$ are N independent identically distributed (i.i.d) samples from $P(\cdot)$. Clearly, $\tilde{L}(\theta)$ is an unbiased estimation of $L(\theta)$. When $g_{\text{tch}}(h_\theta(\lambda)|\lambda)$ is well-behaved [48] for all $\lambda \sim P(\cdot)$, we can have:

$$\begin{aligned} \nabla_\theta L(\theta) &= \nabla_\theta E_{\lambda \sim P(\cdot)}[g_{\text{tch}}(h_\theta(\lambda)|\lambda)] \\ &= E_{\lambda \sim P(\cdot)} \nabla_\theta [g_{\text{tch}}(h_\theta(\lambda)|\lambda)] \end{aligned} \quad (8)$$

where the expectation and differentiation are swapped. Then

$$\nabla_\theta \tilde{L}(\theta) = \frac{1}{N} \sum_{i=1}^N \nabla_\theta [g_{\text{tch}}(h_\theta(\lambda^i)|\lambda^i)] \quad (10)$$

can be used for approximating $\nabla_\theta L(\theta)$.

For each fixed λ , $\nabla_\theta [g_{\text{tch}}(h_\theta(\lambda)|\lambda)]$ can be computed using the chain rule:

$$\nabla_\theta g_{\text{tch}}(h_\theta(\lambda)|\lambda) = \frac{\partial h_\theta(\lambda)}{\partial \theta} \cdot \nabla_x g_{\text{tch}}(x|\lambda)|_{x=h_\theta(\lambda)}. \quad (11)$$

When $h_\theta(\lambda)$ is a neural network and θ is its parameters as in this paper, the Jacobian matrix $\frac{\partial h_\theta(\lambda)}{\partial \theta}$ can be easily computed via the backpropagation algorithm. A brief illustration of the forward and backward pass of the model can be found in Fig. 1.

We assume that there is no analytic formula exists for computing $\nabla_x g_{\text{tch}}(x|\lambda)$, and thus use a simple evolution strategy (ES) [49], [50], [51] to estimate it. To do so, we first sample K independent n -dimensional standard Gaussian random vector $\{u_1, \dots, u_K\} \sim \mathcal{N}(0, I_n)$, and then approximate $\nabla_x g_{\text{tch}}(x|\lambda)$ by

$$\bar{\nabla}_x g_{\text{tch}}(x|\lambda) = \frac{1}{\sigma K} \sum_{k=1}^K (g_{\text{tch}}(x + \sigma u_k|\lambda) - g_{\text{tch}}(x|\lambda)) \cdot u_k, \quad (12)$$

where $\sigma > 0$ is a control parameter. This gradient approximation method is also related to the Gaussian smoothing approach [52], [53], and more advanced estimation can also be adopted into our framework in future work.

According to the Tchebycheff decomposition (3), the gradeint $\nabla_x g_{\text{tch}}(x|\lambda)$ can also be approximated by:

$$\bar{\nabla}_x g_{\text{tch}}(x|\lambda) = \frac{\lambda_{j^*}}{\sigma K} \sum_{k=1}^K (f_{j^*}(x + \sigma u_k) - f_{j^*}(x)) \cdot u_k, \quad (13)$$

where $j^* = \arg \max_{1 \leq j \leq m} \{\lambda_j(f_j(x) - (z_j^* - \varepsilon))\}$. If there is a tie, it can be broken randomly. This approximation does not require the value for $\{f_j(x + \sigma u_k), \forall j \neq j^*\}$ and can further reduce the evaluation cost if all objective functions are evaluated separately.

It should be noticed that the approximation (12) and (13) are not always the same. According to the definition in the Tchebycheff decomposition (3), when $\{\lambda_j(f_j(x) - (z_j^* - \varepsilon))\}$ have similar values for multiple j , it is possible that $j_1 = \arg \max_{1 \leq j \leq m} \{\lambda_j(f_j(x) - (z_j^* - \varepsilon))\}$ and $j_2 = \arg \max_{1 \leq j \leq m} \{\lambda_j(f_j(x + \sigma u_k) - (z_j^* - \varepsilon))\}$ are for two different objectives. In contrast, $f_{j^*}(x)$ and $f_{j^*}(x + \sigma u_k)$ will always share the same j^* in (13). In this work, we do not leverage the computational advantage of the Tchebycheff

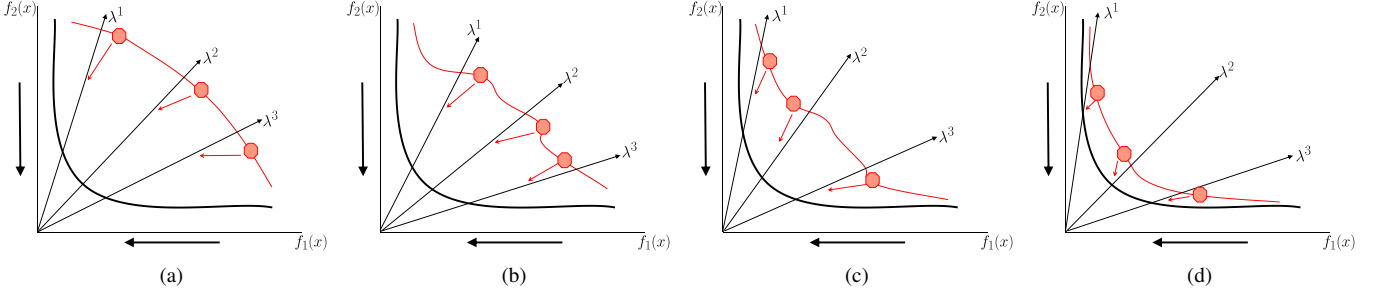


Fig. 2. **Convergence of our Proposed Evolutionary Pareto Set Learning (EPSL) Method:** EPSL gradually pushes the set model to ground truth Pareto set via iteratively reducing the corresponding subproblems values of the sampled solutions. It does **not** require any Pareto-optimal solution just like the traditional MOEA counterparts which gradually push a set of solutions (e.g., population) to the ground truth Pareto set.

Algorithm 1 Evolutionary Stochastic Optimization for EPSL

```

1: Input: Model  $\mathbf{x} = h_{\theta^0}(\boldsymbol{\lambda})$  with Initialized Parameter  $\boldsymbol{\theta}^0$ , Number of MC Samples  $N$ , Number of Gaussian Samples  $K$ 
2: for  $t = 1$  to  $T$  do
3:   Sample  $N$  weight vectors  $\{\boldsymbol{\lambda}^1, \dots, \boldsymbol{\lambda}^N\}$  from  $P(\boldsymbol{\lambda})$ 
4:   Calculate the estimated gradient for each  $\boldsymbol{\lambda}^i$  with  $K$  samples as in (12) and (14)
5:   Update  $\boldsymbol{\theta}^t$  with evolutionary gradient descent as in (15)
6: end for
7: Output: Model  $\mathbf{x} = h_{\theta^T}(\boldsymbol{\lambda})$ 
```

gradient approximation (13), and use the general approximation (12) for all problems.

With the ES-based gradient estimation, we can approximate the gradient for $\tilde{L}(\boldsymbol{\theta})$ by:

$$\bar{\nabla}_{\boldsymbol{\theta}} \tilde{L}(\boldsymbol{\theta}) = \frac{1}{N} \sum_{i=1}^N \frac{\partial h_{\boldsymbol{\theta}}(\boldsymbol{\lambda}^i)}{\partial \boldsymbol{\theta}} \cdot \bar{\nabla}_{\mathbf{x}} g_{\text{tch}}(\mathbf{x} | \boldsymbol{\lambda}^i) |_{\mathbf{x}=h_{\boldsymbol{\theta}}(\boldsymbol{\lambda})}. \quad (14)$$

Let $\boldsymbol{\theta}^t$ be the model parameter at iteration t , we propose to update it with the simple gradient descent:

$$\boldsymbol{\theta}^{t+1} = \boldsymbol{\theta}^t - \eta^t \bar{\nabla}_{\boldsymbol{\theta}} \tilde{L}(\boldsymbol{\theta}^t), \quad (15)$$

where $\eta^t > 0$ is the step size. This can be regarded as a combination of the evolutionary gradient search (EGS) [54], [55] and the stochastic optimization methods [46], [47], [48]. We call this method as Evolutionary Pareto Set learning (EPSL) algorithm and summarize it in **Algorithm 1**.

E. Discussion and Sample Complexity

We could like to make the following remarks on the proposed evolutionary Pareto set learning (EPSL) approach:

- **No Pareto Optimal Solution is Required:** As discussed in the previous subsection, our proposed method learns the set model by gradually minimizing the corresponding objective values for different trade-offs, and does **not** require any Pareto-optimal solutions in advance. For a multi-objective optimization with respect to solution \mathbf{x} , we reformulate it as the set learning problem approach (6) which is an optimization problem with respect to model parameter $\boldsymbol{\theta}$. At each iteration, we randomly sample

N different preferences $\{\boldsymbol{\lambda}_i\}_{i=1}^N$ and use evolutionary stochastic gradient descent to update the model parameter $\boldsymbol{\theta}$. This procedure directly reduces the Tchebycheff aggregated subproblem values $\sum_{i=1}^N g_{\text{tch}}(\mathbf{x} = h_{\boldsymbol{\theta}}(\boldsymbol{\lambda}^i) | \boldsymbol{\lambda}^i)$ with respect to the sampled current corresponding solutions $\mathbf{x}^i = h_{\boldsymbol{\theta}}(\boldsymbol{\lambda}^i)$ predicted by the model as shown in Figure 2, and it does **not** require to explicitly minimize the prediction error between the predicted solutions and the corresponding Pareto-optimal solutions. In this way, we can gradually push our Pareto set model to the ground truth Pareto set without any Pareto-optimal solution.

- **Sample Complexity:** Since our EPSL method does not require any Pareto-optimal solution, the training complexity mainly comes from the function evaluations during the optimization process. If the training objective is convex and differentiable, the complexity of simple first-order gradient descent is $O(\frac{1}{\epsilon})$, which means the number of evaluations (of the gradients) is of the order $O(\frac{1}{\epsilon})$ if we want to obtain an approximate solution with less than ϵ value error to the optimal solution [56]. This complexity is agnostic to the dimension of parameters to optimize (e.g., $\boldsymbol{\theta} \in \mathbb{R}^d$). For a simple zero-order optimization method (such as the simple ES used in this work), the required number of evaluations is $O(\frac{d}{\epsilon})$, which suffers from a factor of d . With advanced methods, the overhead factor can be reduced from d to \sqrt{d} [57], [52]. In EPSL, due to the hierarchical structure as shown in Figure 1, it only needs to estimate the gradient with respect to the decision variable $\mathbf{x} \in \mathbb{R}^n$ rather than the whole model parameters $\boldsymbol{\theta} \in \mathbb{R}^d$ where $n \ll d$ (e.g., $n = 10$ and $d = 10k$). As reported in Table II, EPSL typically only requires about the same computational budget (e.g., number of evaluations and wall-clock runtimes) as in a single run of MOEA/D, while it can learn to approximate the whole Pareto set.

III. STRUCTURE CONSTRAINTS FOR SOLUTION SET

A. Structure Constraints

To incorporate structure constraints on optimal solution sets in multiobjective optimization, we define a general set optimization problem for MOP (1). Let $S \subset \mathcal{X}$ be the set we

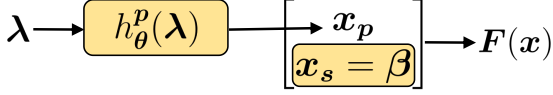


Fig. 3. EPSL Model for solution set with shared components. The variables to optimize are the model parameters θ and part of the decision variables $x_s = \beta$ that shared by all trade-off solutions.

want to find and $Q(S)$ be a quality metric of S with regards to the objective vector $F(\mathbf{x})$, our goal is to

$$\begin{aligned} \min \quad & Q(S), \\ \text{s.t.} \quad & \text{Some constraints on } S. \end{aligned} \quad (16)$$

We call this problem the multiobjective set optimization problem (MSOP). Many existing optimization tasks for dealing with the MOP (1) can be regarded as special cases of the MSOP. Two typical examples are:

- When the constraint on S is that any two different elements in S cannot dominate each other, and Q is the hypervolume of S , the MSOP (16) becomes the problem of finding all the Pareto optimal solutions.
- When the constraint on S is that S can be represent as a Pareto set model (4) and Q is defined as the expected values over all valid subproblems (6), the MSOP (16) is the Pareto set learning problem studied in the above section.

It should be pointed out that some effort has been made to view multiobjective optimization problems as set optimization problems. Particularly, performance indicator based algorithms [58], [59], [60] aim to optimize a performance metric of a solution set with finite solutions. However, they do not consider structure constraints. We consider several typical structure constraints on the whole solution set and hence also on the Pareto set model $h_\theta(\lambda)$ in the following subsections.

B. Shared Component Constraint

To support multiobjective modular design, decision-makers may require that all the solutions in S share some common components. More precisely, let $s \subset \{1, \dots, n\}$, $p = \{1, \dots, n\} \setminus s$, x_s and x_p be the subvector of \mathbf{x} associated with the index sets s and p , respectively. The shared component constraint on S with respect to s is that the x_s -values of all the solutions in S are the same. If we consider this constraint in Paerto set learning (4), then the model can be expressed as

$$x_s = \beta, \quad x_p = h_\theta^p(\lambda) \quad (17)$$

where β and θ are two sets of parameters to learn, h^p is a map from Δ to $R^{|p|}$. The model structure is illustrated in Fig. 3.

For the model with shared component constraint (17), the optimization problem (6) becomes:

$$\min_{\theta, \beta} L(\theta, \beta) = \mathbb{E}_{\lambda \sim P(\lambda)} g_{\text{tch}}(x_s = \beta, x_p = h_\theta^p(\lambda) | \lambda). \quad (18)$$

The gradient of $L(\theta, \beta)$ can be computed as follows:

$$\nabla_\theta L(\theta, \beta) = \mathbb{E}_{\lambda \sim P(\lambda)} \nabla_\theta g_{\text{tch}}(x_s = \beta, x_p = h_\theta^p(\lambda) | \lambda), \quad (19)$$

$$\nabla_\beta L(\theta, \beta) = \mathbb{E}_{\lambda \sim P(\lambda)} \nabla_\beta g_{\text{tch}}(x_s = \beta, x_p = h_\theta^p(\lambda) | \lambda) \quad (20)$$

where

$$\nabla_\theta g_{\text{tch}} = \frac{\partial h_\theta^p(\lambda)}{\partial \theta} \cdot \nabla_{x_p} g_{\text{tch}}([x_s = \beta, x_p = h_\theta^p(\lambda)] | \lambda), \quad (21)$$

$$\nabla_\beta g_{\text{tch}} = \nabla_{x_s} g_{\text{tch}}(\mathbf{x}) |_{x_s = \beta}. \quad (22)$$

It is straightforward to use the proposed evolutionary stochastic optimization method in **Algorithm 1** to optimize θ and β at the same time.

C. Learnable Variable Relationship Constraint

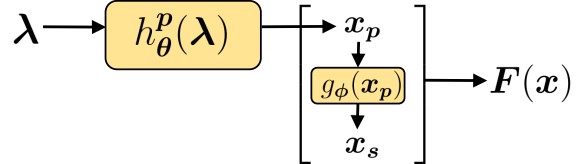


Fig. 4. EPSL Model for solution set with learnable variable relationship constraints. The variables to optimize are the model parameters θ and the learnable relation expression g_ϕ from some base decision variables x_p to the dependent decision variables x_s .

In some real-world applications such as engineering design problems [35], decision-makers may require that the decision variables satisfy some specified relationship. Let x_s and x_p as defined in the previous subsection, we consider the following relationship between x_s and x_p :

$$x_s = g_\phi(x_p), \quad (23)$$

where g is a function with a learnable parameter ϕ , and it characterizes the relationship between x_s and x_p . For example, g can be a linear function as studied in [34].

When the learnable relation structure (23) is considered, the Pareto set model (4) can be expressed as

$$x_s = g_\phi(x_p), \quad x_p = h_\theta^p(\lambda) \quad (24)$$

where ϕ and θ are two sets of parameters to learn. The model structure is illustrated in Fig. 4.

For the model with variable relation constraint (24), the optimization problem (6) becomes:

$$\min_{\theta, \phi} L(\theta, \phi) = \mathbb{E}_{\lambda \sim P(\lambda)} g_{\text{tch}}(x_s = g_\phi(x_p), x_p = h_\theta^p(\lambda) | \lambda). \quad (25)$$

The gradient of $L(\theta, \phi)$ can be computed as follows:

$$\nabla_\theta L(\theta, \phi) = \mathbb{E}_{\lambda \sim P(\lambda)} \nabla_\theta g_{\text{tch}}(g_\phi(h_\theta^p(\lambda)), h_\theta^p(\lambda) | \lambda), \quad (26)$$

$$\nabla_\phi L(\theta, \phi) = \mathbb{E}_{\lambda \sim P(\lambda)} \nabla_\phi g_{\text{tch}}(g_\phi(h_\theta^p(\lambda)), h_\theta^p(\lambda) | \lambda) \quad (27)$$

where

$$\begin{aligned} \nabla_\theta g_{\text{tch}} &= \frac{\partial h_\theta^p(\lambda)}{\partial \theta} \cdot [\nabla_{x_p} g_{\text{tch}}(\mathbf{x} | \lambda) \\ &\quad + \frac{\partial g_\phi(x_p)}{\partial x_p} \nabla_{x_s} g_{\text{tch}}(\mathbf{x} | \lambda)] |_{x_s = g_\phi(x_p), x_p = h_\theta^p(\lambda)}, \end{aligned} \quad (28)$$

$$\nabla_\phi g_{\text{tch}} = \frac{\partial g_\phi(\lambda)}{\partial \phi} \cdot \nabla_{x_s} g_{\text{tch}}(\mathbf{x} | \lambda) |_{x_s = g_\phi(x_p), x_p = h_\theta^p(\lambda)}. \quad (29)$$

Our proposed evolutionary stochastic optimization method in **Algorithm 1** can be directly used to optimize θ and ϕ .

D. Shape Structure Constraint

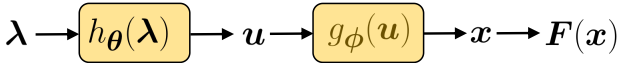


Fig. 5. EPSL Model for solution set with shape structure constraint. The variables to optimize are the model parameters θ and the parameters ϕ for the shape function $g_\phi(\mathbf{u})$.

In some multiobjective problems, the decision-makers may require that the solution set has an intrinsic low-dimensional structure or a pre-defined shape. For this purpose, we introduce the compositional set model with shape function g_ϕ :

$$\mathbf{u}(\lambda) = h_\theta(\lambda), \quad \mathbf{x} = g_\phi(\mathbf{u}(\lambda)), \quad (30)$$

where $\mathbf{u} \in \mathbb{R}^d$ is a latent embedding with dimension $d \leq m-1$, and θ, ϕ are the model parameters to optimize. Fig. 5 illustrates the set model architecture with such shape structure constraints. In this model, the essential dimensionality of the solution set can be the same as that of μ , and its geometrical shape is determined by the function g_ϕ .

With the shape structure constraints, we have the following optimization problem for set model learning:

$$\min_{\theta, \phi} L(\theta, \phi) = \mathbb{E}_{\lambda \sim P(\lambda)} g_{\text{tch}}(\mathbf{x} = g_\phi(h_\theta(\lambda)) | \lambda). \quad (31)$$

The gradients of $L(\theta, \phi)$ with respect to the parameters θ and ϕ are:

$$\nabla_\theta L(\theta, \phi) = \mathbb{E}_{\lambda \sim P(\lambda)} \nabla_\theta g_{\text{tch}}(\mathbf{x} = g_\phi(h_\theta(\lambda)) | \lambda), \quad (32)$$

$$\nabla_\phi L(\theta, \phi) = \mathbb{E}_{\lambda \sim P(\lambda)} \nabla_\phi g_{\text{tch}}(\mathbf{x} = g_\phi(h_\theta(\lambda)) | \lambda) \quad (33)$$

where

$$\nabla_\theta g_{\text{tch}} = \frac{\partial h_\theta(\lambda)}{\partial \theta} \cdot \left[\frac{\partial g_\phi(\mathbf{u})}{\partial \mathbf{u}} \nabla_\mathbf{u} g_{\text{tch}}(\mathbf{x} | \lambda) \right] |_{\mathbf{x} = g_\phi(h_\theta(\lambda))}, \quad (34)$$

$$\nabla_\phi g_{\text{tch}} = \frac{\partial g_\phi(\mathbf{u})}{\partial \phi} \cdot \nabla_\mathbf{u} g_{\text{tch}}(\mathbf{x} | \lambda) |_{\mathbf{x} = g_\phi(h_\theta(\lambda))}. \quad (35)$$

The parameters θ and ϕ can be optimized with **Algorithm 1**.

The form of shape function $g_\phi(\mathbf{x})$ can be provided by decision-makers to model their requirement. One possible application is to use a simple and explicit expression to approximate the solution set for supporting decision making. In this paper, we consider a simple polygonal chain structure for bi-objective optimization problem, and leave the investigation on other shape structures to future work.

The polygonal chain (or piecewise linear curve) is a simple way to approximate a space curve for capturing its skeleton [61], [62], [63]. A polygonal chain P_c with $K - 1$ line segments can be defined by a sequence of knee points $[\mathbf{p}_1, \mathbf{p}_2, \dots, \mathbf{p}_K]$ called its vertices and a location parameter $t \in [0, K]$ called the tracer. A solution on P_c with tracer t can be represented by:

$$\mathbf{x} = \mathbf{p}_k + (t - k)(\mathbf{p}_{k+1} - \mathbf{p}_k), \text{ if } t \in [k, k+1] \quad (36)$$

for $k = 1, 2, \dots, K$. It is straightforward to incorporate the polygonal chain structure into our proposed set model as illustrated in Fig. 6. Now we have:

$$t = h_\theta(\lambda)$$

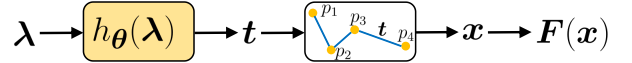


Fig. 6. EPSL Model for the solution set with learnable polygonal chain. The variables to optimize are the model parameters θ for the tracer $t_\theta(\lambda)$, and the locations for a sequence of vertices $[\mathbf{p}_1, \mathbf{p}_2, \dots, \mathbf{p}_K]$.

$$\begin{aligned} \mathbf{x} &= g_\phi(t) = \mathbf{p}_k + (t(\lambda) - k)(\mathbf{p}_{k+1} - \mathbf{p}_k), \\ &\text{if } t(\lambda) \in [k, k+1] \end{aligned} \quad (37)$$

for $k = 1, 2, \dots, K$. The tracer $t = h_\theta(\lambda)$ is the learnable latent embedding of the solution set, and the shape function $g_\phi(\cdot)$ is fully parameterized by the learnable vertices $[\mathbf{p}_1, \mathbf{p}_2, \dots, \mathbf{p}_K]$. Once the approximate solution set is obtained, it can be fully reconstructed with the K vertices $[\mathbf{p}_1, \mathbf{p}_2, \dots, \mathbf{p}_K]$ where the number K is usually small in practice. Decision-makers can readily find any preferred solutions by assigning their preference λ .

IV. EXPERIMENTAL STUDIES

We first compare EPSL with classical MOEAs on 16 real-world multiobjective engineering design problems, and then investigate EPSL's ability to deal with structure constraints on the whole solution set.

A. Experimental Settings

1) Optimization Problems: The multiobjective engineering design optimization test instance suite (RE problems) proposed in [1]¹ are used in our experimental studies. This instance suite contains 16 different real-world engineering design problems with 2, 3, 4, 6 and 9 optimization objectives from various domains such as bar truss design [64] and car cab design [65]. These problems have different properties and shapes of the Pareto front. A detailed summary of these problems can be found in [1].

2) Algorithm Setting: Our proposed EPSL method has a strong connection to the decomposition-based algorithms. In this section, we compare it with three representative decomposition-based and preference-based MOEA, namely MOEA/D [31] with Tchebycheff (MOEA/D-TCH) and PBI decomposition (MOEA/D-PBI), NSGA-III [65], as well as the seminal dominance-based NSGA-II [66]. We implement all MOEAs with the open-sourced pymoo [67]² and our proposed EPSL³ with PyTorch [68].

All methods are given the same number of function evaluations for each problem, which is 26,000 for two objective problems, and 41,000 for problems with three or more objectives. Following the experiment settings in [1], all MOEAs have the population size 100, 105, 120, 182 and 210 for problems with 2, 3, 4, 6 and 9 objectives, respectively. The evolutionary operators are SBX crossover and polynomial mutation for all MOEAs, and we use the default settings for other parameters as in their original papers.

¹<https://github.com/ryojitanabe/reproblems>

²<https://pymoo.org/index.html>

³Will be open-sourced upon publication.

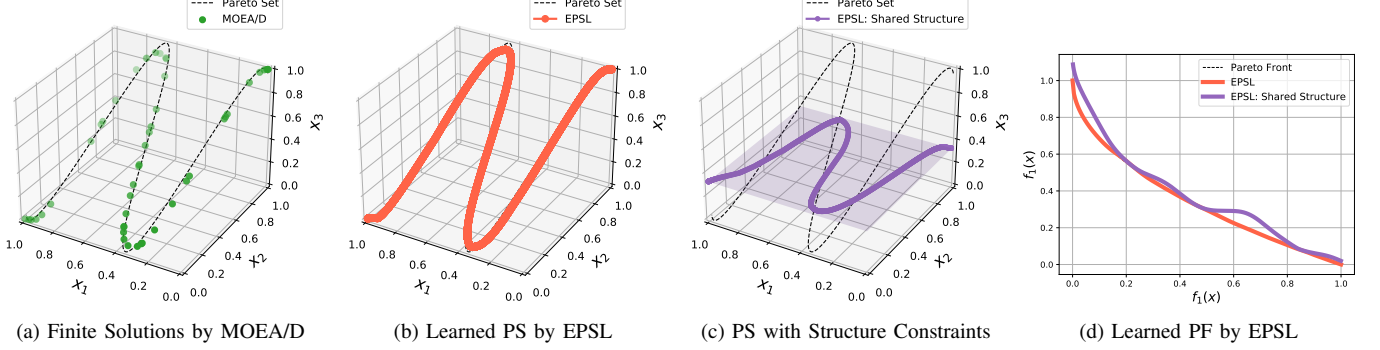


Fig. 7. **Set of Finite Solutions and the Learned Pareto Set:** (a) MOEA/D can only find a set of finite solutions to approximate the Pareto set. (b) The proposed EPSL can successfully approximate the whole Pareto set that contains infinite number of solutions. (c) EPSL can easily incorporate structure constraints on the learned solution set. Here all solutions on the constrained solution set share the same x_3 . (d) The corresponding Pareto fronts in the objective space. Decision-makers can directly obtain any preferred solutions in real time by exploring the learned Pareto set without further optimization step. For this problem, the learned Pareto front with a shared solution structure is only slightly outperformed by the unconstrained Pareto front.

TABLE I
PERFORMANCE OF EPSL WITH DIFFERENT MODEL STRUCTURES.

Size	Single Hidden Layer			Two Hidden Layers			Three Hidden Layers		
	64	512	1024	64-64	512-512 (this work)	1024-1024	64-64-64	512-512-512	1024-1024-1024
RE21	1.29e-02	1.28e-02	1.16e-02	1.01e-02	2.26e-03	2.21e-03	8.70e-03	2.24e-03	2.32e-03
RE33	3.41e-02	5.51e-03	4.02e-03	1.57e-02	1.44e-03	1.03e-03	1.19e-02	9.88e-04	9.91e-04

TABLE II
AVERAGE RUN TIME FOR OPTIMIZATION AND SAMPLING ON PROBLEMS WITH DIFFERENT NUMBERS OF OBJECTIVES.

# Eval.	MOEA/D	EPSL	100 Samples	1,000 Samples
RE21	26,000	16.4s	15.8s	+0.00s
RE31	41,000	26.2s	25.9s	+0.00s
RE41	41,000	30.1s	30.8s	+0.00s
RE61	41,000	28.7s	27.2s	+0.01s
RE91	41,000	33.8s	37.5s	+0.01s

Our proposed EPSL is trained by the lightweight evolutionary stochastic gradient optimization method proposed in Section II-D. It randomly samples 5 (for two objective problems) or 8 (for other problems) valid preferences at each iteration, and samples 5 solutions to estimate the gradient for each preference. The total number of iterations is 1,000 for all problems. At the end of optimization, we randomly sample 100 to 210 (match those for MOEAs) or 1,000 preferences and obtain their corresponding Pareto solutions for comparison with other MOEAs. Therefore, the total number of evaluations is at most 26,000 and 41,000 for problems with 2 and 3 or more objectives, respectively. The average running times for problems with different numbers of objectives are reported in Table II. With the proposed efficient stochastic evolutionary gradient descent algorithm, EPSL is comparable with MOEA/D in terms of running time on all test instances. In addition, sampling solutions from the learned Pareto set is trivial and their computational cost can be neglected.

3) *Performance Indicator:* We use hypervolume (HV) [69] as the performance indicator, and report the hypervolume difference (Δ HV) with the approximated Pareto front provided

by [1] for each algorithm. To calculate the hypervolume values, we first normalize all obtained solutions into the unit space $[0, 1]^m$ with the approximated ideal point z^{ideal} and nadir point z^{nadir} provided in [1], and then calculate the hypervolume values with reference vector $(1.1, \dots, 1.1)^m$. We run each algorithm 21 times for each problem and report the median value. For each comparison, we conduct a Wilcoxon rank-sum test at the 5% significance level and calculate the performance score [60] for each algorithm.

4) *Model Setting for EPSL:* In this work, we use a simple model and find it works well for all problems without specific tuning. We have conducted an experimental analysis on our proposed EPSL method with different model structures on the RE21 and RE33 problems as shown in Table I. The best and close to best results are highlighted in **bold**. According to the results, a very small model (e.g., those with a single hidden layer) does not have enough capacity to learn the whole Pareto set, and hence has a poor performance. On the other hand, once the model has sufficient capacity, further increasing the model size will not lead to significantly better performance.

B. Simple Synthetic Problem

We first consider the following synthetic two-objective optimization problem to illustrate the properties of EPSL:

$$\begin{aligned} & \min_{\mathbf{x} \in [0,1], \mathbf{x}_{[2:n]} \in [-1,1]^{n-1}} (f_1(\mathbf{x}), f_2(\mathbf{x})), \text{ where} \\ & f_1(\mathbf{x}) = \mathbf{x}_1, \\ & f_2(\mathbf{x}) = (1+g)(1 - \sqrt{\mathbf{x}_1/(1+g)}), \\ & g = \frac{1}{n-1} \sum_{i=2}^n (\mathbf{x}_i - \sin(10(\mathbf{x}_1 - 0.5)))^2, \end{aligned} \quad (38)$$

TABLE III

THE MEDIAN HYPERVOLUME GAP ($\Delta HV \downarrow$) OF 21 INDEPENDENT RUNS ON 16 RE PROBLEMS. THE (+/-) SYMBOLS INDICATE EPSL IS SIGNIFICANTLY BETTER THAN/EQUAL TO/WORSE THAN THE CORRESPONDING ALGORITHM. WE REPORT THE PERFORMANCE SCORES IN THE PARENTHESIS, AND HIGHLIGHT THE BEST RESULTS IN BOLD AND GREY BACKGROUND.

	NSGA-II	NSGA-III	MOEA/D-TCH	MOEA/D-PBI	EPSL	EPSL(1000)
RE21-Four Bar Truss Design	7.46e-03 (5) +	5.02e-03 (2) +	4.93e-03 (1) +	7.01e-03 (3) +	6.94e-03 (3) +	2.26e-03 (0)
RE22-Reinforced Concrete Beam Design	7.32e-03 (2) -	6.10e-03 (1) -	5.72e-03 (0) -	8.84e-03 (3) -	3.32e-02 (5) +	1.08e-02 (4)
RE23-Pressure Vessel Design	1.32e-03 (1) +	2.51e-03 (3) +	4.09e-03 (4) +	4.78e-03 (5) +	1.21e-03 (1) +	1.52e-04 (0)
RE24-Hatch Cover Design	2.39e-03 (1) +	3.79e-03 (2) +	3.77e-03 (2) +	1.16e-02 (5) +	3.79e-03 (2) +	4.93e-04 (0)
RE25-Coil Compression Spring Design	5.59e-04 (2) +	6.24e-03 (3) +	6.18e-03 (3) +	1.68e-02 (5) +	4.29e-08 (0) =	4.29e-08 (0)
RE31-Two Bar Truss Design	7.65e-05 (4) +	1.06e-05 (2) +	7.40e-05 (3) +	5.36e-04 (5) +	6.68e-06 (1) +	3.48e-06 (0)
RE32-Welded Beam Design	2.83e-03 (2) +	1.19e-02 (3) +	1.18e-02 (3) +	3.48e-02 (5) +	2.19e-04 (1) +	1.95e-04 (0)
RE33-Disc Brake Design	1.39e-01 (5) +	2.96e-02 (2) +	5.52e-02 (3) +	7.02e-02 (4) +	2.07e-02 (1) +	1.44e-03 (0)
RE34-Vehicle Crashworthiness Design	2.42e-02 (0) -	3.83e-02 (1) -	4.28e-02 (2) -	6.36e-02 (3) -	8.36e-02 (5) +	7.99e-02 (4)
RE35-Speed Reducer Design	9.89e-03 (3) +	1.10e-02 (4) +	4.96e-03 (2) +	1.02e-02 (4) +	4.26e-03 (1) +	2.46e-03 (0)
RE36-Gear Train Design	3.25e-03 (2) +	1.74e-02 (5) +	7.86e-03 (3) +	8.95e-03 (4) +	1.48e-03 (1) +	3.90e-04 (0)
RE37-Rocket Injector Design	6.00e-02 (4) +	5.68e-02 (4) +	3.91e-02 (1) +	4.45e-02 (3) +	4.34e-02 (2) +	1.60e-02 (0)
RE41-Car Side Impact Design	1.42e-01 (4) +	1.38e-01 (4) +	9.71e-02 (3) +	8.89e-02 (2) +	8.50e-02 (1) +	4.59e-02 (0)
RE42-Conceptual Marine Design	1.66e-02 (2) +	6.67e-02 (4) +	4.38e-03 (1) +	3.23e-02 (3) +	1.68e-02 (2) +	4.11e-03 (0)
RE61-Water Resource Planning	1.16e-01 (3) +	1.42e-01 (5) +	9.44e-02 (2) +	1.31e-01 (4) +	1.27e-02 (1) +	-9.37e-03 (0)
RE91-Car Cab Design	3.51e-02 (2) +	3.63e-02 (3) +	2.28e-02 (0) -	4.98e-02 (5) +	4.54e-02 (4) +	3.42e-02 (1)
+/-	14/0/2	14/0/2	13/0/3	14/0/2	15/1/0	-
Average Score	2.625	3.000	2.0625	3.9375	1.9375	0.5625

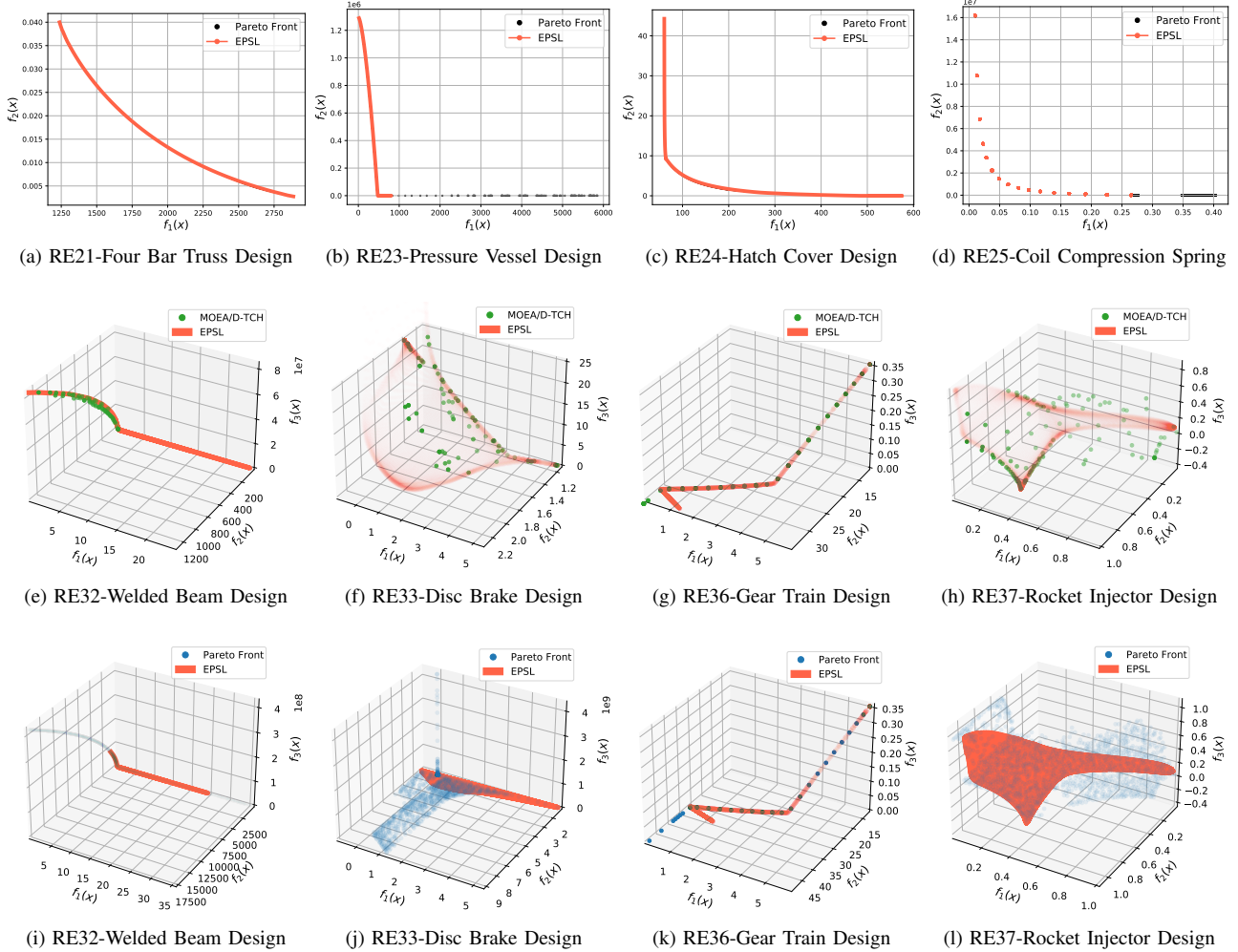


Fig. 8. **The Learned Pareto Front for RE Problems:** (a)-(d) EPSL is able to learn the Pareto front for bi-objective problems. (e)-(h) For the three objective optimization problems, EPSL allows the decision-makers to easily explore different trade-off solutions on the learned Pareto front, while MOEA/D can only provide a set of finite solutions. (i)-(l) Compared with the approximated Pareto front with exhausted search by different methods, EPSL can learn the part of Pareto front with critical trade-offs, but it might fail to find the regions which mainly contain weakly Pareto efficient solutions.

TABLE IV
PERFORMANCE OF EPSL WITH WEIGHTED-SUM (WS), PENALTY BOUNDARY INTERSECTION (PBI), AND TCHEBYCHEFF (TCH) AGGREGATION METHODS.
WE REPORT BOTH THE RESULTS WITH 100 AND 1,000 SAMPLES.

	EPSL-WS	100 Samples			1,000 Samples		
		EPSL-PBI	EPSL-TCH	EPSL-WS	EPSL-PBI	EPSL-TCH	
RE21-Four Bar Truss Design	1.53e-02	5.46e-03	6.94e-03	2.02e-03	1.45e-03	2.26e-03	
RE22-Reinforced Concrete Beam Design	1.22e-01	2.78e-02	3.32e-02	2.65e-02	8.14e-03	1.08e-02	
RE23-Pressure Vessel Design	2.17e-02	1.13e-02	1.21e-03	1.46e-02	3.64e-03	1.52e-04	
RE24-Hatch Cover Design	1.98e-01	1.93e-01	3.79e-03	1.98e-01	1.93e-01	4.93e-04	
RE25-Coil Compression Spring Design	7.91e-03	8.23e-05	4.29e-08	8.08e-05	4.69e-05	4.29e-08	
RE31-Two Bar Truss Design	1.17e-04	3.70e-05	6.68e-06	7.71e-05	2.93e-05	3.48e-06	
RE32-Welded Beam Design	3.08e-03	2.98e-03	2.19e-04	2.57e-03	2.48e-03	1.95e-04	
RE33-Disc Brake Design	6.90e-02	1.28e-02	2.07e-02	1.97e-02	1.03e-03	1.44e-03	
RE34-Vehicle Crashworthiness Design	2.30e-01	2.31e-01	8.36e-02	2.22e-01	2.19e-01	7.99e-02	
RE35-Speed Reducer Design	6.18e-02	6.35e-02	4.26e-03	5.64e-02	5.79e-02	2.46e-03	
RE36-Gear Train Design	1.89e-02	8.16e-04	1.48e-03	9.87e-04	-8.16e-03	3.90e-04	
RE37-Rocket Injector Design	1.79e-01	7.00e-02	4.34e-02	3.59e-02	2.93e-02	1.60e-02	
RE41-Car Side Impact Design	2.18e-01	7.04e-02	8.50e-02	6.58e-02	4.41e-02	4.59e-02	
RE42-Conceptual Marine Design	9.22e-01	1.46e-02	1.68e-02	6.35e-01	2.99e-03	4.11e-03	
RE61-Water Resource Planning	2.11e-02	-2.32e-03	1.27e-02	-1.04e-03	-1.25e-02	-9.37e-03	
RE91-Car Cab Design	5.54e-02	5.09e-02	4.54e-02	4.12e-02	3.76e-02	3.42e-02	
+/-	16/0/0	9/0/7	-	16/0/0	9/0/7	-	

where its Pareto optimal set is a sine-like curve. From the results shown in Fig. 7(a)(b), it is clear that EPSL can approximate the whole Pareto set while classic MOEA can only find a finite set of solutions. With the learned Pareto set model, decision-makers can easily adjust their preferences and explore the corresponding solutions on the approximate Pareto set in real time without extra optimization steps. In Fig. 7(c)(d), a structure constraint on the whole solution set is further incorporated into EPSL. We require all solutions should share the same component x_3 whose optimal value is unknown in advance. It is clear that EPSL can successfully learn the solution set with such structure constraints.

C. Unconstrained Pareto Set Learning

The experimental results on hypervolume difference (ΔHV) for 16 different real-world multiobjective engineering design problems (RE problems) [1] are shown in Table. III. Our proposed EPSL method can approximate the whole Pareto set for a given problem via a single model, which is significantly different from a fixed finite set of solutions obtained by other MOEAs. With the learned Pareto set model, we can randomly sample an arbitrary number of solutions from the learned Pareto set and calculate its hypervolume difference. In Table. III, we report the results of two sampled solution sets by EPSL. The first one (e.g., named EPSL) has the same number of solutions with other algorithms, which is used for a fair comparison (e.g., from 100 to 210 for different problems with 2 to 9 objectives). We also report the results for a dense solution set with 1,000 solutions (e.g., named EPSL(1000)) to show the extra advantage of our approach. It should be noticed that the total number of evaluations for EPSL is either smaller than (with the regular set) or equal (with the dense set) to other MOEAs in comparison. The computational overhead is trivial for the solutions sampling as reported in Table. II.

According to the results in Table. III, EPSL performs comparably with MOEA/D-TCH with the same number of solutions, which is expected. By further sampling more solutions on the learned Pareto set, EPSL can significantly outperform all

other MOEAs on most test instances. The promising ability to approximate the whole Pareto set makes EPSL become a flexible alternative to the traditional MOEAs.

Some Pareto fronts learned by EPSL are shown in Fig. 8. For the two objective problems, EPSL can well approximate the major part of the Pareto front for all the test instances, except the part of weakly Pareto optimal solutions (RE23 and RE25). For the three objective problems, we compare EPSL with MOEA/D-TCH and the Pareto set provided in [1], which is obtained from multiple exhaustive searches of different algorithms with a significantly larger number of evaluations. Compared to MOEA/D-TCH, EPSL can learn a significantly large part of the Pareto front than a set of finite solutions. On the dense Pareto front, although EPSL will sometimes miss the part of weakly Pareto optimal solutions, it can fully explore the major part of the Pareto front with significant and meaningful trade-offs. In this work, we mainly focus on developing the key idea to learn the whole Pareto set, and thus use a simple model and optimization algorithm for EPSL. It is worth investigating more powerful models and optimization algorithms to further improve the performance of EPSL in future work.

D. EPSL with Different Aggregation Methods

In this work, we focus on the Tchebycheff (TCH) aggregation due to its good theoretical properties. We now also conduct experiments on EPSL with the widely-used weighted-sum (WS) and the penalty boundary intersection (PBI) aggregation methods as shown in Table. IV. According to the results, EPSL-WS performs poorly on most problems, while EPSL-PBI has a similar overall performance compared with EPSL-TCH. These results are reasonable since EPSL is a model-based extension and shares many properties similar to MOEA/D. For example, the simple weighted-sum (WS) aggregation cannot find any non-convex parts of the Pareto front and hence will lead to poor overall performance. How to properly select the most suitable aggregation method for each specific problem is still an open question for MOEA/D and also for EPSL (e.g., PBI and TCH are good at different problems).

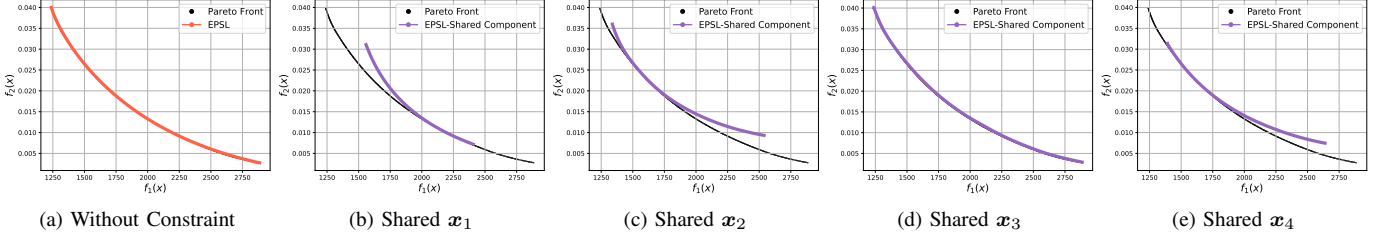


Fig. 9. **The Learned Solution Set for the Four Bar Truss Design Problem (RE21) with Shared Components:** (a) The learned Pareto front without structure constraint. (b)-(e) The image of solution set where the decision variable x_1 , x_2 , x_3 , x_4 (the lengths of four bars) are shared respectively.

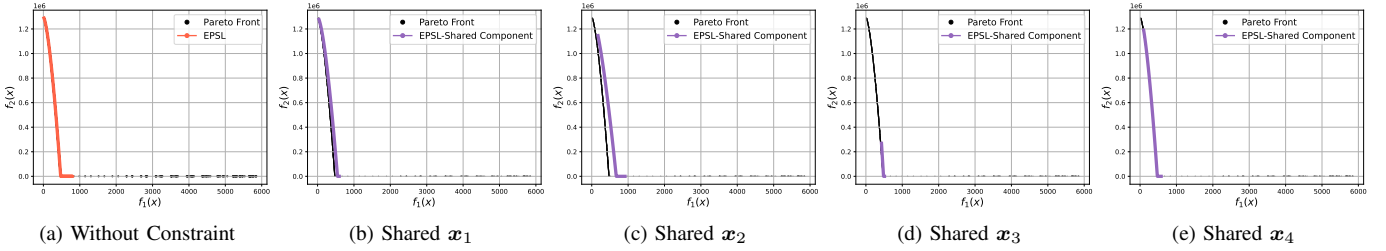


Fig. 10. **The Learned Solution Set for the Pressure Vessel Design Problem (RE23) with Shared Components:** (a) The learned Pareto front without structure constraint. (b)-(e) The image of learned solution set where the decision variable x_1 (thicknesses of the shell), x_2 (head of a pressure vessel), x_3 (inner radius), x_4 (length of the cylindrical section) are shared respectively.

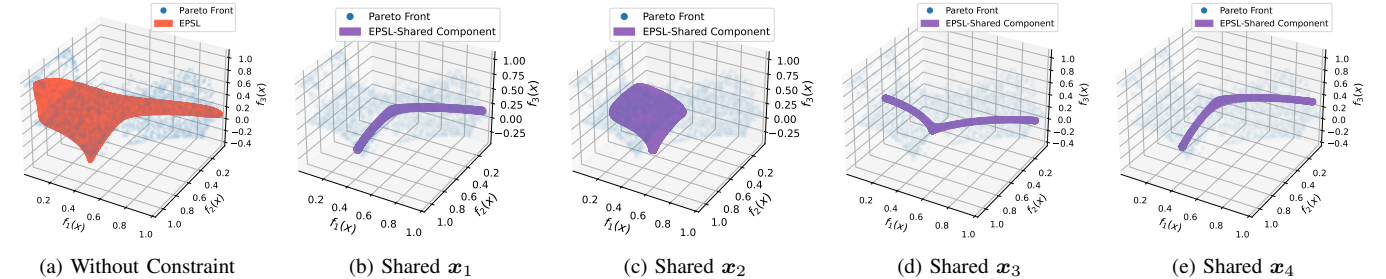


Fig. 11. **The Learned Solution Set for the Rocket Injector Design Problem (RE37) with Shared Components:** (a) The learned Pareto front without structure constraint. (b)-(e) The image of learned solution set where the decision variable x_1 (hydrogen flow angle), x_2 (hydrogen area), x_3 (oxygen area), x_4 (oxidizer post tip thickness) are shared respectively.

E. Optimal Set with Shared Components

To validate the ability of EPSL to learn the optimal solution set with shared components, we conduct experiments on three different engineering design problems. For the four bar truss design problem (RE21) [70], we learn the optimal solution sets with a shared length of different bars (x_1, x_2, x_3, x_4) as shown in Fig. 9. For the pressure vessel design problem (RE23) [71], we consider the optimal solution sets that share thickness of the shell (x_1), head of a pressure vessel (x_2), inner radius (x_3), or length of the cylindrical section (x_4) respectively as shown in Fig. 10. For the rocket injector design problem (RE37) [72], the solution set with shared hydrogen flow angle (x_1), hydrogen area (x_2), oxygen area (x_3), or oxidizer post tip thickness (x_4) is learned as shown in Fig. 11. The results clearly show that EPSL can successfully learn the solution sets with various shared component constraints.

By sharing different components, each learned solution set has its own structure and is quite different from the others. For some applications, the solution sets with shared components

might perform in a similar way to the unconstrained Pareto set, such as sharing the length of a specific bar for the four bar truss design (e.g., Fig. 9(d)). In other cases, the shared component might lead to degenerate or sometimes significantly worsen the performance. We believe these learned solution sets can provide valuable knowledge to support informative decision making. The decision-makers can now trade off the Pareto optimality with their desirable structure constraints.

F. EPSL with Learnable Variable Relationship

We investigate EPSL's ability to learn an optimal solution set with a predefined and learnable variable relationship for the synthetic optimization problem and the real-world four-bar truss design problem (RE21) [70].

For the synthetic optimization problem (38), the optimal Pareto set satisfies the following formulation:

$$\mathbf{x}_i = \sin(10(\mathbf{x}_1 - 0.5)), \quad \forall i \in [2, \dots, n] \quad (39)$$

which is unknown for the algorithm. Decision-makers typically have a finite set of approximate solutions with traditional

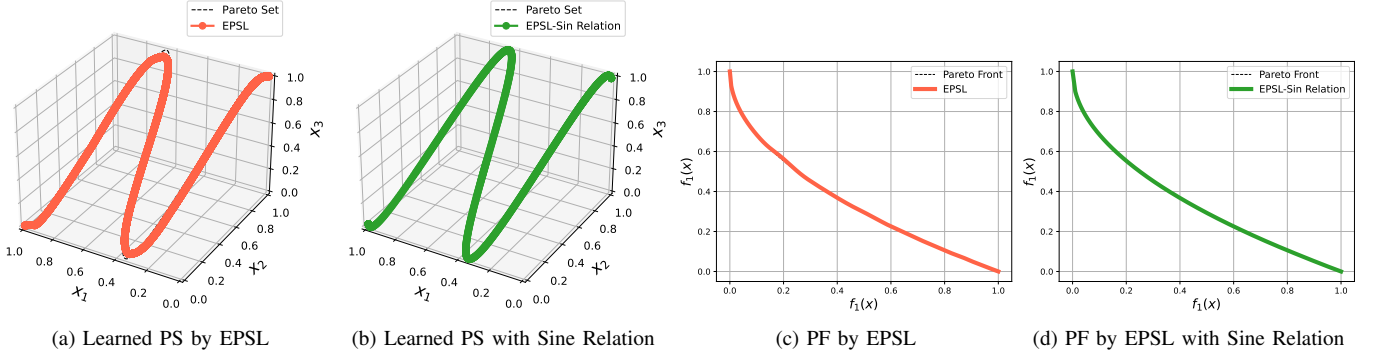


Fig. 12. **EPSL with Learnable Sine-Curve Relationship for the Synthetic Optimization Problem:** (a) The approximate Pareto set learned by the original EPSL. (b) The approximate Pareto set with learnable sine-curve relation. (c) The approximate Pareto front obtained by the original EPSL. (d) The approximate Pareto front corresponds to the learned Pareto set with the sine-curve structure.

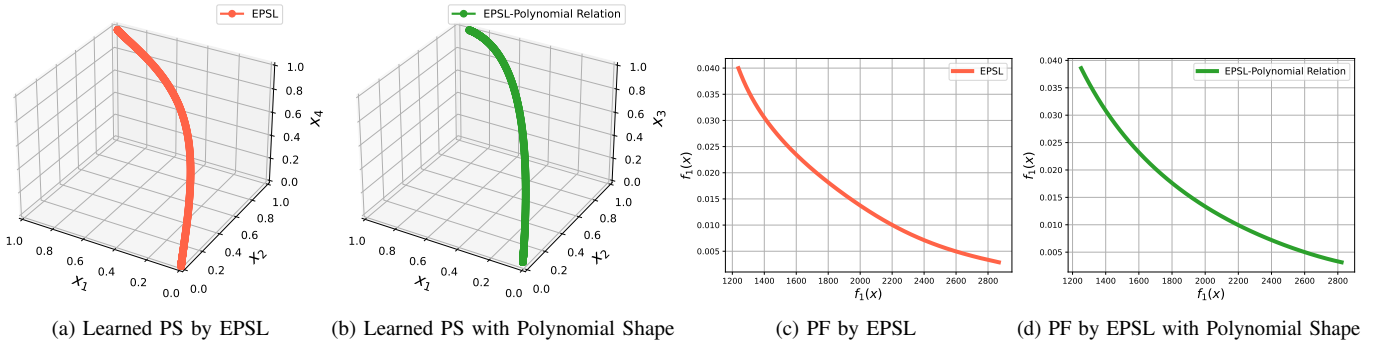


Fig. 13. **EPSL with Learnable Polynomial Relationship for the Four Bar Truss Design Problem:** (a) The approximate Pareto set learned by the original EPSL. (b) The approximate Pareto set with learnable polynomial relation. (c) The approximate Pareto front obtained by the original EPSL. (d) The approximate Pareto front corresponds to the learned Pareto set with the polynomial structure.

MOEAs (e.g., Fig. 7(a)) or a somehow black-box model-based Pareto set approximation with the original EPSL (e.g., Fig. 12(a)).

Suppose some prior knowledge of the Pareto set, such as the sine-curve-like structure, is available (e.g., via preliminary investigation), we can directly incorporate them into the Pareto set modeling:

$$\begin{aligned} \mathbf{x}_1 &= h_{\theta}^P(\boldsymbol{\lambda}), \\ \mathbf{x}_i &= \sin(\alpha_i(\mathbf{x}_1 - \beta_i)), \forall i \in [2, \dots, n], \end{aligned} \quad (40)$$

where $h_{\theta}^P(\boldsymbol{\lambda})$ is the Pareto set model with learnable parameter θ and $\mathbf{x}_i = \sin(\alpha_i(\mathbf{x}_1 - \beta_i))$ is the predefined variable relationship with learnable parameters α and β . The parameters $[\theta, \alpha, \beta]$ can be easily optimized by our proposed evolutionary stochastic optimization method in **Algorithm 1**. According to the results shown in Figure 12, the learned Pareto set can match the ground truth Pareto set while providing more useful information (e.g., the explicit parametric formulation) for the given problem. This extra information could be useful to support more informative decision-making.

For the real-world four-bar truss design problem, the formulation of ground truth Pareto set is completely unknown. In this case, we propose a simple polynomial formulation to approximate the Pareto set:

$$\mathbf{x}_1 = h_{\theta}^P(\boldsymbol{\lambda}),$$

$$\mathbf{x}_i = 1 - \alpha_i(\mathbf{x}_1 - \beta_i)^2, \forall i \in [2, \dots, n]. \quad (41)$$

By optimizing the learnable parameters $[\theta, \alpha, \beta]$, we obtain the parametric Pareto set approximation as in Figure 13. While the learned simple parametric Pareto set is not identical to the unconstrained approximate Pareto set by the original EPSL, their corresponding Pareto fronts are very similar to each other. With a similar optimization performance, the much simpler parametric solution set could be preferred for practical decision-making.

G. EPSL with Shape Structure Constraint

This subsection demonstrates the ability of EPSL to learn a Pareto set with a simple polygonal chain structure. We set the number of vertices $K = 4$ for all problems, and compare its performance with the unconstrained EPSL. The learned Pareto sets and the corresponding Pareto front on the synthetic problem (38) and the four bar truss design problem (RE21) are shown in Fig. 14. According to the results, EPSL with polygonal chain constraints can find a solution set with a much simpler structure, while its corresponding Pareto front performs slightly worse.

We also report the hypervolume difference (ΔHV) and IGD+ values [73] for other bi-objective engineering design problems in Table V. These results show that EPSL can find a reasonably good approximation to the ground truth Pareto set

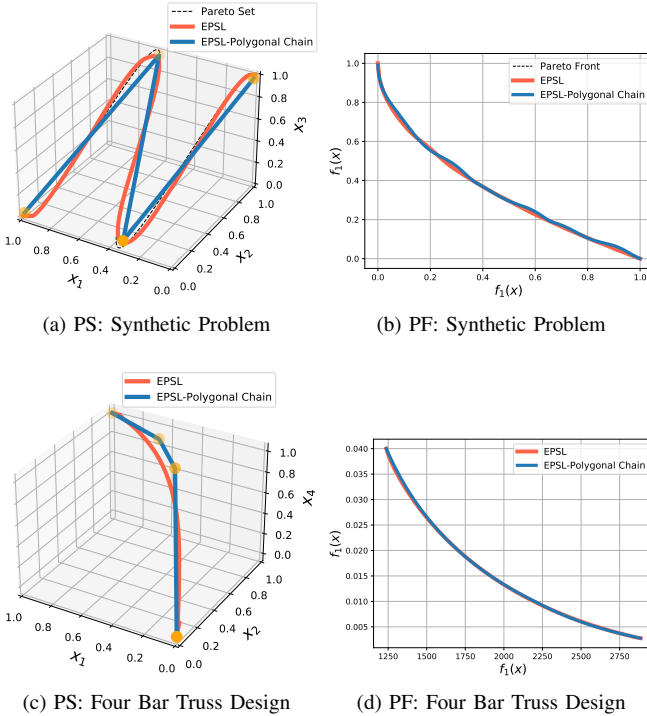


Fig. 14. EPSL with Polygonal Chain Structure Constraints: (a)(c) EPSL can successfully learn the polygonal chains with crucial vertices to well approximate the ground truth Pareto sets. (b)(d) Even though the constrained Pareto sets have much simpler structures, their corresponding Pareto fronts can provide nearly comparable trade-offs with the ground truth Pareto fronts.

TABLE V
THE MEDIAN HYPERVOLUME GAP (ΔHV) AND IGD+ VALUES OF EPSL
WITH AND WITHOUT POLYGONAL CHAIN STRUCTURE. SIGNIFICANTLY
BETTER RESULTS ARE HIGHLIGHTED IN BOLD, AND SIMILAR RESULTS ARE
MARKED BY UNDERLINING.

	EPSL-Polygonal Chain		EPSL	
	ΔHV	IGD+	ΔHV	IGD+
Syn	8.42e-03	6.04e-03	3.67e-03	1.79e-03
RE21	8.23e-03	4.79e-03	2.26e-03	1.57e-03
RE22	7.06e-02	4.46e-02	1.08e-02	6.32e-03
RE23	5.08e-02	2.83e-02	1.52e-04	2.27e-04
RE24	1.93e-01	1.03e-01	4.93e-04	3.56e-04
RE25	4.22e-01	8.72e-02	4.29e-08	1.24e-07

with a much simpler polygonal chain structure. A simple Pareto set with an explainable structure, instead of a complicated one, could be much easier to understand and can shed insights into the optimization problem at hand. In some applications, decision-makers could prefer such a simple Pareto set while it might be trade-offed with the absolute Pareto optimality. Our proposed EPSL can well support this demand.

V. DISCUSSION AND CONCLUSION

This paper has proposed a novel evolutionary Pareto set learning (EPSL) method to approximate the whole Pareto set for continuous multiobjective optimization problems. The proposed method generalizes the two major components of MOEA/D, namely decomposition and collaboration, with the learning-based model. For decomposition, EPSL generalizes the scalarization approach from a fixed and finite set of

preferences to consider all infinite valid preferences via a single neural network model. For collaboration, we propose an efficient evolutionary stochastic gradient search method to optimize the learned Pareto set concerning all preferences simultaneously. The knowledge and information are now shared among all preferences within the same model, rather than exchanged among a fixed set of finite subproblems. In addition, the proposed EPSL method can easily incorporate different structure constraints on the whole solution set for multiobjective optimization. It allows decision-makers to trade off the optimal objective values with desirable properties on the solution set, which goes beyond the classic Pareto optimality for multiobjective optimization.

In terms of computational overhead, our proposed EPSL is about the same as a single run of MOEA/D, while it allows decision makers to choose any trade-off solutions on the whole learned Pareto set. We believe it is a promising alternative to the traditional MOEAs, and can lead to many interesting applications and algorithms. In this paper, we focus on the key idea of learning the whole Pareto set via a single model, and keep the model and optimization algorithm simple and straightforward. Many important improvements should be investigated in future work:

- Building more powerful models to approximate complicated Pareto sets, such as those with discrete decision variables, disconnected structures, or complex patterns.
- Proposing more efficient optimization methods for learning the Pareto set model, which should go beyond the straightforward Monte-Carlo sampling and simple evolutionary gradient descent.
- Generalizing EPSL to tackle different optimization scenarios such as expensive optimization, interactive optimization, and dynamic optimization.

REFERENCES

- [1] R. Tanabe and H. Ishibuchi, “An easy-to-use real-world multi-objective optimization problem suite,” *Applied Soft Computing*, vol. 89, p. 106078, 2020.
- [2] X. Lin, H.-L. Zhen, Z. Li, Q. Zhang, and S. Kwong, “Pareto multi-task learning,” in *Advances in Neural Information Processing Systems*, 2019, pp. 12 060–12 070.
- [3] Z. Lu, G. Sreekumar, E. Goodman, W. Banzhaf, K. Deb, and V. N. Boddeti, “Neural architecture transfer,” *IEEE Transactions on Pattern Analysis and Machine Intelligence (TPAMI)*, 2021.
- [4] C. Hillermeier, “Generalized homotopy approach to multiobjective optimization,” *Journal of Optimization Theory and Applications*, vol. 110, no. 3, pp. 557–583, 2001.
- [5] Q. Zhang, A. Zhou, and Y. Jin, “Rm-med: A regularity model-based multiobjective estimation of distribution algorithm,” *IEEE Transactions on Evolutionary Computation*, vol. 12, no. 1, pp. 41–63, 2008.
- [6] M. Ehrgott, *Multicriteria optimization*. Springer Science & Business Media, 2005, vol. 491.
- [7] K. Miettinen, *Nonlinear multiobjective optimization*. Springer Science & Business Media, 2012.
- [8] E. Zitzler, *Evolutionary algorithms for multiobjective optimization: Methods and applications*. Citeseer, 1999, vol. 63.
- [9] K. Deb, *Multi-Objective Optimization Using Evolutionary Algorithms*. New York, NY, USA: John Wiley & Sons, Inc., 2001.
- [10] A. Zhou, B.-Y. Qu, H. Li, S.-Z. Zhao, P. N. Suganthan, and Q. Zhang, “Multiobjective evolutionary algorithms: A survey of the state of the art,” *Swarm and Evolutionary Computation*, vol. 1, no. 1, pp. 32–49, 2011.
- [11] J. Knowles, “Parego: A hybrid algorithm with on-line landscape approximation for expensive multiobjective optimization problems,” *IEEE Transactions on Evolutionary Computation*, vol. 10, no. 1, pp. 50–66, 2006.

- [12] Q. Zhang, W. Liu, E. Tsang, and B. Virginas, "Expensive multiobjective optimization by moea/d with gaussian process model," *IEEE Transactions on Evolutionary Computation*, vol. 14, no. 3, pp. 456–474, 2010.
- [13] T. Chugh, Y. Jin, K. Miettinen, J. Hakanen, and K. Sindhya, "A surrogate-assisted reference vector guided evolutionary algorithm for computationally expensive many-objective optimization," *IEEE Transactions on Evolutionary Computation*, vol. 22, no. 1, pp. 129–142, 2016.
- [14] M. Wu, K. Li, S. Kwong, Q. Zhang, and J. Zhang, "Learning to decompose: A paradigm for decomposition-based multiobjective optimization," *IEEE Transactions on Evolutionary Computation*, vol. 23, no. 3, pp. 376–390, 2018.
- [15] Y. Liu, H. Ishibuchi, N. Masuyama, and Y. Nojima, "Adapting reference vectors and scalarizing functions by growing neural gas to handle irregular pareto fronts," *IEEE Transactions on Evolutionary Computation*, vol. 24, no. 3, pp. 439–453, 2019.
- [16] Q. Liu, Y. Jin, M. Heiderich, T. Rodemann, and G. Yu, "An adaptive reference vector-guided evolutionary algorithm using growing neural gas for many-objective optimization of irregular problems," *IEEE Transactions on Cybernetics*, 2020.
- [17] K. Shang, W. Chen, W. Liao, and H. Ishibuchi, "Hv-net: Hypervolume approximation based on deepsets," *IEEE Transactions on Evolutionary Computation*, 2022.
- [18] K. Shang, W. Liao, and H. Ishibuchi, "Hvc-net: Deep learning based hypervolume contribution approximation," in *International Conference on Parallel Problem Solving from Nature*. Springer, 2022, pp. 414–426.
- [19] J. Rakowska, R. T. Haftka, and L. T. Watson, "Tracing the efficient curve for multi-objective control-structure optimization," *Computing Systems in Engineering*, vol. 2, no. 5-6, pp. 461–471, 1991.
- [20] M. Hartikainen, K. Miettinen, and M. M. Wieeek, "Constructing a pareto front approximation for decision making," *Mathematical Methods of Operations Research*, vol. 73, no. 2, pp. 209–234, 2011.
- [21] I. Giagkiozis and P. J. Fleming, "Pareto front estimation for decision making," *Evolutionary computation*, vol. 22, no. 4, pp. 651–678, 2014.
- [22] R. Cheng, Y. Jin, K. Narukawa, and B. Sendhoff, "A multiobjective evolutionary algorithm using gaussian process-based inverse modeling," *IEEE Transactions on Evolutionary Computation*, vol. 19, no. 6, pp. 838–856, 2015.
- [23] X. Lin, Z. Yang, and Q. Zhang, "Pareto set learning for neural multi-objective combinatorial optimization," in *Proc. International Conference on Learning Representations (ICLR)*, 2022.
- [24] X. Lin, Z. Yang, X. Zhang, and Q. Zhang, "Pareto set learning for expensive multiobjective optimization," in *Proc. Advances in Neural Information Processing Systems (NeurIPS)*, 2022.
- [25] P. Guo, Q. Zhang, and X. Lin, "Approximation of a pareto set segment using a linear model with sharing variables," in *International Conference on Evolutionary Multi-Criterion Optimization*. Springer, 2023, pp. 247–259.
- [26] X. Lin, Z. Yang, X. Zhang, and Q. Zhang, "Continuation path learning for homotopy optimization," in *Proc. International Conference on Machine Learning (ICML)*. PMLR, 2023, pp. 21288–21311.
- [27] X. Lin, Z. Yang, Q. Zhang, and S. Kwong, "Controllable pareto multi-task learning," *arXiv preprint arXiv:2010.06313*, 2020.
- [28] A. Navon, A. Shamsian, G. Chechik, and E. Fetaya, "Learning the Pareto front with hypernetworks," in *Proc. International Conference on Learning Representations (ICLR)*, 2021.
- [29] M. Ruchte and J. Grabocka, "Scalable pareto front approximation for deep multi-objective learning," in *2021 IEEE International Conference on Data Mining (ICDM)*. IEEE, 2021, pp. 1306–1311.
- [30] M. Jain, S. C. Raparthi, A. Hernandez-Garcia, J. Rector-Brooks, Y. Bengio, S. Miret, and E. Bengio, "Multi-objective gflownets," *arXiv preprint arXiv:2210.12765*, 2022.
- [31] Q. Zhang and H. Li, "MOEA/D: A multiobjective evolutionary algorithm based on decomposition," *IEEE Transactions on evolutionary computation*, vol. 11, no. 6, pp. 712–731, 2007.
- [32] R. Rai and V. Allada, "Modular product family design: agent-based pareto-optimization and quality loss function-based post-optimal analysis," *International Journal of Production Research*, vol. 41, no. 17, pp. 4075–4098, 2003.
- [33] K. Sinha and E. S. Suh, "Pareto-optimization of complex system architecture for structural complexity and modularity," *Research in Engineering Design*, vol. 29, no. 1, pp. 123–141, 2018.
- [34] K. Deb, "Unveiling innovative design principles by means of multiple conflicting objectives," *Engineering Optimization*, vol. 35, no. 5, pp. 445–470, 2003.
- [35] K. Deb and A. Srinivasan, "Innovation: Innovating design principles through optimization," in *Proceedings of the 8th annual conference on Genetic and evolutionary computation*, 2006, pp. 1629–1636.
- [36] K. Deb, S. Bandaru, D. Greiner, A. Gaspar-Cunha, and C. C. Tutum, "An integrated approach to automated innovation for discovering useful design principles: Case studies from engineering," *Applied Soft Computing*, vol. 15, pp. 42–56, 2014.
- [37] S. Bandaru, T. Aslam, A. H. Ng, and K. Deb, "Generalized higher-level automated innovation with application to inventory management," *European Journal of Operational Research*, vol. 243, no. 2, pp. 480–496, 2015.
- [38] R. Guha and K. Deb, "Regemo: Sacrificing pareto-optimality for regularity in multi-objective problem-solving," in *International Conference on Evolutionary Multi-Criterion Optimization*. Springer, 2023, pp. 29–42.
- [39] I. Das and J. E. Dennis, "Normal-boundary intersection: A new method for generating the pareto surface in nonlinear multicriteria optimization problems," *SIAM journal on optimization*, vol. 8, no. 3, pp. 631–657, 1998.
- [40] H.-L. Liu, F. Gu, and Q. Zhang, "Decomposition of a multiobjective optimization problem into a number of simple multiobjective subproblems," *IEEE transactions on evolutionary computation*, vol. 18, no. 3, pp. 450–455, 2013.
- [41] R. Wang, Z. Zhou, H. Ishibuchi, T. Liao, and T. Zhang, "Localized weighted sum method for many-objective optimization," *IEEE Transactions on Evolutionary Computation*, vol. 22, no. 1, pp. 3–18, 2016.
- [42] S. Jiang, S. Yang, Y. Wang, and X. Liu, "Scalarizing functions in decomposition-based multiobjective evolutionary algorithms," *IEEE Transactions on Evolutionary Computation*, vol. 22, no. 2, pp. 296–313, 2017.
- [43] V. J. Bowman, "On the relationship of the tchebycheff norm and the efficient frontier of multiple-criteria objectives," in *Multiple criteria decision making*. Springer, 1976, pp. 76–86.
- [44] E. U. Choo and D. Atkins, "Proper efficiency in nonconvex multicriteria programming," *Mathematics of Operations Research*, vol. 8, no. 3, pp. 467–470, 1983.
- [45] H. Li and Q. Zhang, "Multiobjective optimization problems with complicated pareto sets, moea/d and nsga-ii," *IEEE transactions on evolutionary computation*, vol. 13, no. 2, pp. 284–302, 2009.
- [46] H. Robbins and S. Monro, "A stochastic approximation method," *The annals of mathematical statistics*, pp. 400–407, 1951.
- [47] L. Bottou *et al.*, "Online learning and stochastic approximations," *On-line learning in neural networks*, vol. 17, no. 9, p. 142, 1998.
- [48] A. Nemirovski, A. Juditsky, G. Lan, and A. Shapiro, "Robust stochastic approximation approach to stochastic programming," *SIAM Journal on optimization*, vol. 19, no. 4, pp. 1574–1609, 2009.
- [49] N. Hansen and A. Ostermeier, "Completely derandomized self-adaptation in evolution strategies," *Evolutionary computation*, vol. 9, no. 2, pp. 159–195, 2001.
- [50] H.-G. Beyer and H.-P. Schwefel, "Evolution strategies—a comprehensive introduction," *Natural computing*, vol. 1, no. 1, pp. 3–52, 2002.
- [51] Z. Li, X. Lin, Q. Zhang, and H. Liu, "Evolution strategies for continuous optimization: A survey of the state-of-the-art," *Swarm and Evolutionary Computation*, vol. 56, p. 100694, 2020.
- [52] Y. Nesterov and V. Spokoiny, "Random gradient-free minimization of convex functions," *Foundations of Computational Mathematics*, vol. 17, no. 2, pp. 527–566, 2017.
- [53] K. Gao and O. Sener, "Generalizing gaussian smoothing for random search," in *Proc. International Conference on Machine Learning (ICML)*, 2022.
- [54] R. Salomon, "Evolutionary algorithms and gradient search: similarities and differences," *IEEE Transactions on Evolutionary Computation*, vol. 2, no. 2, pp. 45–55, 1998.
- [55] D. V. Arnold and R. Salomon, "Evolutionary gradient search revisited," *IEEE Transactions on Evolutionary Computation*, vol. 11, no. 4, pp. 480–495, 2007.
- [56] Y. Nesterov, *Introductory lectures on convex optimization: A basic course*. Springer Science & Business Media, 2003, vol. 87.
- [57] J. C. Duchi, M. I. Jordan, M. J. Wainwright, and A. Wibisono, "Optimal rates for zero-order convex optimization: The power of two function evaluations," *IEEE Transactions on Information Theory*, vol. 61, no. 5, pp. 2788–2806, 2015.
- [58] E. Zitzler and S. Künzli, "Indicator-based selection in multiobjective search," in *International conference on parallel problem solving from nature*. Springer, 2004, pp. 832–842.
- [59] N. Beume, B. Naujoks, and M. Emmerich, "Sms-emoa: Multiobjective selection based on dominated hypervolume," *European Journal of Operational Research*, vol. 181, no. 3, pp. 1653–1669, 2007.
- [60] J. Bader and E. Zitzler, "Hype: An algorithm for fast hypervolume-based many-objective optimization," *Evolutionary computation*, vol. 19, no. 1, pp. 45–76, 2011.

- [61] R. Bellman, "On the approximation of curves by line segments using dynamic programming," *Communications of the ACM*, vol. 4, p. 284, 1961.
- [62] J. G. Dunham, "Optimum uniform piecewise linear approximation of planar curves," *IEEE Transactions on Pattern Analysis and Machine Intelligence*, pp. 67–75, 1986.
- [63] P. L. Rosin, "Techniques for assessing polygonal approximations of curves," *IEEE Trans. Pattern Anal. Mach. Intell.*, vol. 19, pp. 659–666, 1997.
- [64] C. C. Coello and G. T. Pulido, "Multiobjective structural optimization using a microgenetic algorithm," *Structural and Multidisciplinary Optimization*, vol. 30, no. 5, pp. 388–403, 2005.
- [65] K. Deb and H. Jain, "An evolutionary many-objective optimization algorithm using reference-point-based nondominated sorting approach, part i: solving problems with box constraints," *IEEE transactions on evolutionary computation*, vol. 18, no. 4, pp. 577–601, 2013.
- [66] K. Deb, A. Pratap, S. Agarwal, and T. Meyarivan, "A fast and elitist multiobjective genetic algorithm: Nsga-ii," *IEEE transactions on evolutionary computation*, vol. 6, no. 2, pp. 182–197, 2002.
- [67] J. Blank and K. Deb, "pymoo: Multi-objective optimization in python," *IEEE Access*, vol. 8, pp. 89497–89509, 2020.
- [68] A. Paszke, S. Gross, F. Massa, A. Lerer, J. Bradbury, G. Chanan, T. Killeen, Z. Lin, N. Gimelshein, L. Antiga *et al.*, "Pytorch: An imperative style, high-performance deep learning library," *Advances in neural information processing systems*, vol. 32, pp. 8026–8037, 2019.
- [69] E. Zitzler and L. Thiele, "Multiobjective evolutionary algorithms: a comparative case study and the strength pareto approach," *IEEE transactions on Evolutionary Computation*, vol. 3, no. 4, pp. 257–271, 1999.
- [70] F. Cheng and X. Li, "Generalized center method for multiobjective engineering optimization," *Engineering Optimization*, vol. 31, no. 5, pp. 641–661, 1999.
- [71] S. Kramer, "An augmented lagrange multiplier based method for mixed integer discrete continuous optimization and its applications to mechanical design," *Journal of Mechanical Design*, vol. 116, p. 405, 1994.
- [72] R. Vaidyanathan, K. Tucker, N. Papila, and W. Shyy, "Cfd-based design optimization for single element rocket injector," in *41st Aerospace Sciences Meeting and Exhibit*, 2003, p. 296.
- [73] H. Ishibuchi, H. Masuda, Y. Tanigaki, and Y. Nojima, "Modified distance calculation in generational distance and inverted generational distance," in *International conference on evolutionary multi-criterion optimization*. Springer, 2015, pp. 110–125.